A Cell-Based Constitutive Relation for Bio-Artificial Tissues

George I. Zahalak,*† Jessica E. Wagenseil,* Tetsuro Wakatsuki,‡ and Elliot L. Elson‡
Departments of *Biomedical Engineering, †Mechanical Engineering, and ‡Biochemistry and Molecular Biophysics, Washington University, St. Louis, Missouri 63130 USA

ABSTRACT By using a combination of continuum and statistical mechanics we derive an integral constitutive relation for bio-artificial tissue models consisting of a monodisperse population of cells in a uniform collagenous matrix. This constitutive relation quantitatively models the dependence of tissue stress on deformation history, and makes explicit the separate contribution of cells and matrix to the mechanical behavior of the composite tissue. Thus microscopic cell mechanical properties can be deduced via this theory from measurements of macroscopic tissue properties. A central feature of the constitutive relation is the appearance of "anisotropy tensors" that embody the effects of cell orientation on tissue mechanics. The theory assumes that the tissues are stable over the observation time, and does not in its present form allow for cell migration, reorientation, or internal remodeling. We have compared the predictions of the theory to uniaxial relaxation tests on fibroblast-populated collagen matrices (FPMs) and find that the experimental results generally support the theory and yield values of fibroblast contractile force and stiffness roughly an order of magnitude smaller than, and viscosity comparable to, the corresponding properties of active skeletal muscle. The method used here to derive the tissue constitutive equation permits more sophisticated cell models to be used in developing more accurate representations of tissue properties.

INTRODUCTION

A fundamental problem in physiology is to understand how the cells and matrix that comprise a tissue determine its mechanical properties. A clear and quantitative description of this relationship is important not only for basic biological science, but also for the rational design of artificial tissues. This paper describes the first stage of a theory that accounts for the mechanical properties of a tissue model in terms of its cellular and matrix components. Tissue models reconstituted from specified cells and matrix provide a powerful and flexible experimental approach to this subject (Bell et al., 1979). We have developed methods for producing the model tissues and for measuring their structural and mechanical characteristics (Kolodney and Elson, 1993, 1995; Wakatsuki et al., 2000). Although model tissues are readily assembled using a variety of cell types, including smooth, skeletal, and cardiac muscle (Eschenhagen et al., 1997) and epi and endothelial cells (Kolodney and Wysolmerski, 1992), we focus here on fibroblast-populated matrices (FPMs) in which primary chicken embryo fibroblasts are embedded in a collagen matrix. Measurement of dynamic uniaxial stress-strain relations reveals the mechanical characteristics of these cell-matrix composites and how they depend on factors such as the fabrication procedure, cell concentration, cell type, and drugs or toxins that affect the cytoskeleton and extracellular matrix.

The mechanical interaction of cells and matrix in a tissue, either natural or artificial, is complex and cannot be comprehended adequately in an obvious or intuitive way. Extracellular matrix is a viscoelastic material generating stresses dependent on the history of deformation, and the embedded cells also exhibit viscoelastic behavior in addition to developing active contractile forces. How these constituents combine to determine the mechanical behavior of the composite tissue depends not only on their individual mechanical properties, but also on how they are assembled and connected within the tissue. Models have been proposed to account for specific systems. Among the earliest were constitutive relations for tissues containing mesenchymal (Murray et al., 1983; Murray and Oster, 1984) and epithelial (Odell et al., 1981) cells. The objective of this work was to analyze pattern formation in continuum mechanical theories of morphogenesis; little detail on the mechanics of individual cells was included. More recently, Tranquillo and colleagues have extended the Murray-Oster constitutive relations to build sophisticated models of artificial-tissue mechanics during tissue formation, a process analogous to wound healing (Tranquillo and Murray, 1992, 1993; Moon and Tranquillo, 1993; Barocas et al., 1995; Tranquillo, 1999). The salient mechanical event in this process is a large contraction of the collagen gel with a concomitant expulsion of water (syneresis). In its latest formulation the tissue is represented as a two-phase fluid-solid system, which permits improved predictions of the remodeling dynamics (Barocas and Tranquillo, 1997).

In this paper we will focus on how the mechanical properties of a fully formed tissue model with relatively time-independent properties depend on its cellular and matrix components. We will not treat the fabrication phase of tissue compaction and remodeling. We will build a constitutive equation relating stress and strain history that can be interpreted quantitatively in terms of the mechanical properties of cellular and matrix components. In the first part of this

Received for publication 28 February 2000 and in final form 31 July 2000.
Address reprint requests to Dr. George I. Zahalak, Dept. of Mechanical Engineering, Washington University, Campus Box 1185, One Brookings Dr., St. Louis, MO 63130-4899. Tel.: 314-935-6053; Fax: 314-935-4014; E-mail: giz@me.wustl.edu.

0006-3495/00/11/2369/13 $2.00

paper we describe the general mechanical response of individual cells by a generally accepted physiological model of contractile systems, and then assemble the tissue constitutive relation by averaging over the cell distribution. The moduli appearing in the resulting macroscopic constitutive relation can be interpreted directly in terms of the moduli of the matrix and those of cellular constituents. To the best of our knowledge there is now no other tissue constitutive model that aspires to this level of detail. In the second part of the paper we make a first application of our theory to the analysis of relaxation tests and present experimental results to validate the theory.

DEVELOPMENT OF THE CONSTITUTIVE RELATION

As a point of departure we consider the structure of an FPM after it is formed—that is, after incubation, extrusion of fluid, compaction, and remodeling by the embedded cells. Fig. 1 exhibits micrographs of FPMs containing different concentrations of fibroblasts. Two features appear in this figure that are particularly relevant for constitutive modeling. First, the fibroblasts are spread and elongated, roughly resembling rods with a typical length of 100 μm and a thickness of 10 μm. Second, the direction of these "rods" is

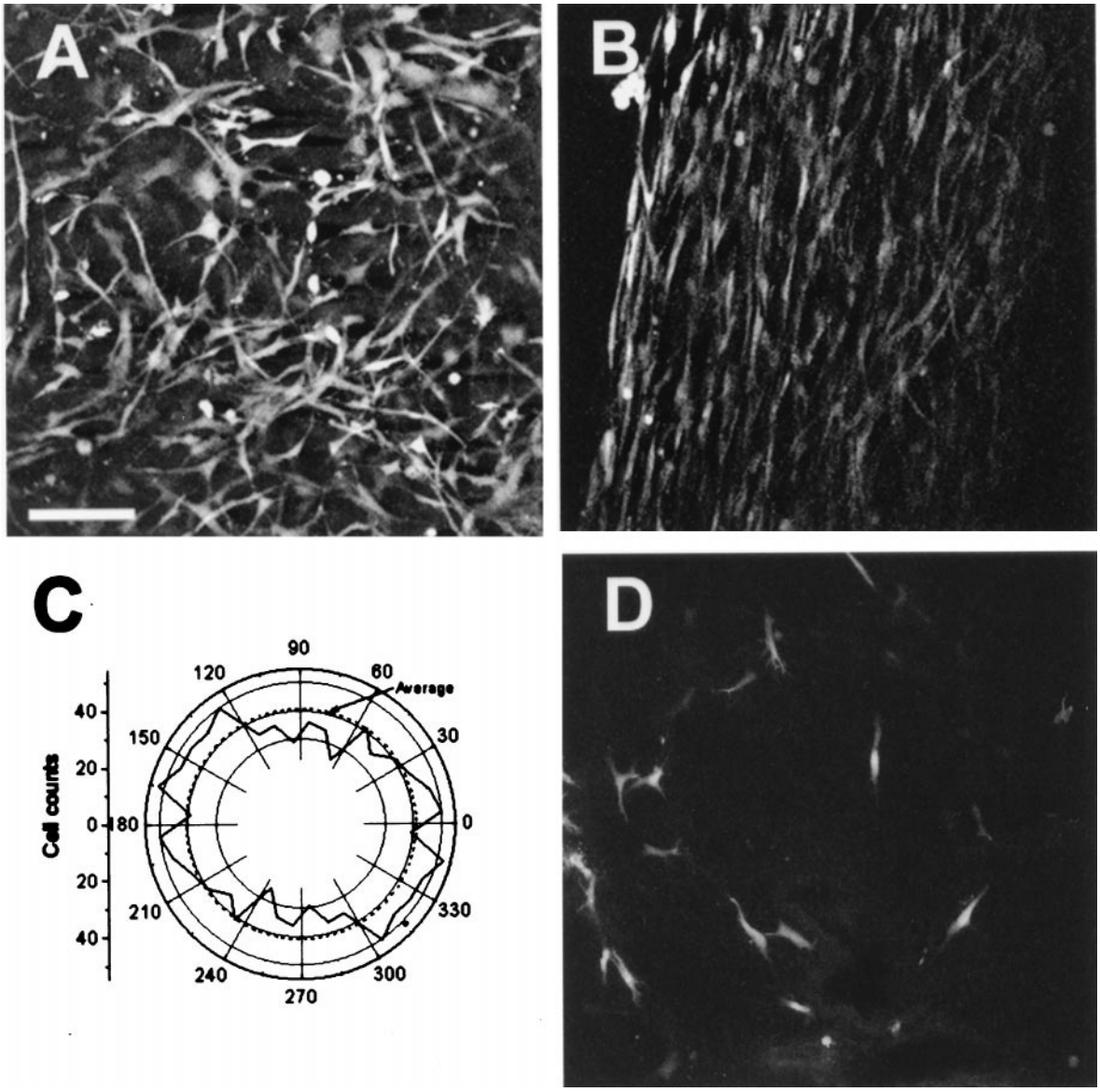

FIGURE 1 (*A*, *B*, *D*) Optical sections of formed tissue models. The cell concentration in *A* and *B* is 1.0×10^6 cells/ml of uncompacted tissue. *A* is in the central region of the sample and *B* is near the edge. *D* is in the central region of a sparse tissue model, with a cell concentration of 0.1×10^6 cells/ml of uncompacted tissue. *C* shows a polar histogram of 720 cell-orientation measurements, partitioned into 10° bins; also shown is the circle representing the average number per bin. (The cell numbers were counted over the range 0° to 180°, and were extended to the range 180°–360° by reflection through the origin.)

variable; in some regions the cells tend to be aligned in one direction (Fig. 1 *B*) whereas in others the cell orientations appear to be random (Fig. 1 *A*). Both of these features figure prominently in the ensuing constitutive relation.

If an imaginary cutting plane, with unit normal n_i, is passed through a point in the FPM, the force per unit area exerted on the material on the negative side (the side from which n_i emanates) by the material on the positive side (the side into which n_i points) is called the traction acting at the point, t_i, and is related to the (Cauchy) stress, σ_{ij}, by $t_j = dA_i\sigma_{ij}$, where $dA_i = n_i dA$ is an area element in the cutting plane. We assume that the traction at any point can be decomposed into the sum of a part associated with the collagen matrix, $t_i^{(m)}$, and a part associated with the cells, $t_i^{(c)}$; thus $t_i = t_i^{(m)} + t_i^{(c)}$. This is equivalent to assuming that the stress at any point is the sum of matrix and cell contributions:

$$\sigma_{ij} = \sigma_{ij}^{(m)} + \sigma_{ij}^{(c)} \tag{1}$$

We proceed further by defining $\sigma_{ij}^{(m)}$ to be the stress that would exist in the FPM, subjected to any specific loading history, if the cell forces were reduced to zero (which can be achieved experimentally by the application of appropriate drugs). The cell stress $\sigma_{ij}^{(c)}$ is assumed to be due to the actual forces exerted by cells intersecting the cutting plane. While there is no physical necessity for the such an additive decomposition to be strictly true (see Discussion), similar assumptions have been made in previous models of tissue mechanics (Murray et al., 1983; Murray and Oster, 1984; Tranquillo and Murray, 1992) and we will adopt it here.

Tissues and tissue models are usually compliant and may be subjected to large deformations. In our own experiments, however, the FPMs are subjected to (engineering) strains not exceeding 20%. In this first version of our constitutive theory we wish to avoid the mathematical complexity of large-deformation kinematics, so we assume that the deformations of the tissue are adequately characterized by the small-strain tensor

$$\varepsilon_{ij} = \tfrac{1}{2}\,(u_{i,j} + u_{j,i}) \tag{2}$$

where u_i is the macroscopic continuum displacement of the tissue and $u_{i,j} = \partial u_i/\partial x_j$.

We assume that the collagen matrix is a passive, homogeneous, isotropic, nonlinear, viscoelastic continuum, and we characterize it by a quasi-linear integral constitutive relation that appears to be particularly appropriate for biological materials (Fung, 1993)

$$\sigma_{ij}^{(m)}(t) = \int_{-\infty}^{t} \lambda(t-\hat{t})\delta_{ij}d\sigma_{kk}^{(e)}(\hat{t}) + 2\int_{-\infty}^{t} \mu(t-\hat{t})d\sigma_{ij}^{(e)}(\hat{t}) \tag{3}$$

where $\lambda(t)$ and $\mu(t)$ are viscoelastic relaxation functions characterizing the matrix. (The distortional relaxation modulus at constant volume is $\mu(t)$ and the volumetric relaxation modulus is $\lambda(t) + (2/3)\,\mu(t)$). The so-called "elastic" stress, $\sigma_{ij}^{(e)}$, is a prescribed function of strain derivable from a strain-energy function, $W(\varepsilon_{ij})$. Thus

$$\sigma_{ij}^{(e)} = \frac{\partial W}{\partial \varepsilon_{ij}} \tag{4}$$

There is some flexibility in the definition of $\sigma_{ij}^{(e)}$. We choose to define it as a dimensionless variable, and assign the physical dimensions of stress to the relaxation functions μ and λ; this implies that the strain energy, W, is also dimensionless. The integral constitutive relation of Eq. 3 is for a *compressible* material, and involves two relaxation functions. If the material is *incompressible* the first integral is replaced by $-p\delta_{ij}$, where p is an isotropic pressure contribution to the stress (which is not determined by the deformation, but rather by the boundary conditions); that is

$$\sigma_{ij}(t) = -p(t)\delta_{ij} + 2\int_{-\infty}^{t} \mu(t-\hat{t})d\sigma_{ij}^{(e)}(\hat{t}) \tag{5}$$

which involves only one relaxation function, $\mu(t)$.

Motivated by the nonlinear uniaxial stress-strain response of FPMs observed in our experiments, we propose the following specific strain-energy function for the elastic stress

$$W(\varepsilon_{ij}) = \frac{3}{2}\varepsilon_0^2\left(e^{\bar{\varepsilon}/\varepsilon_0} - \frac{\bar{\varepsilon}}{\varepsilon_0}\right) \tag{6}$$

where the strain invariant $\bar{\varepsilon} = \sqrt{\tfrac{2}{3}\varepsilon_{ij}\varepsilon_{ij}}$ is known as the "effective strain," or "strain intensity," in continuum constitutive theories (Freudenthal, 1966). (For homogeneous uniaxial deformation of an incompressible material it is easy to show that $\bar{\varepsilon}$ is numerically equal to the axial strain, which facilitates the interpretation of uniaxial experiments in terms of three-dimensional constitutive relations.) This strain-energy function reproduces the behavior observed in our experiments: stress-strain relations that are linear at small strain and exponential at larger strain. Equation 6 contains one material parameter, ε_0, that must be determined from experiments; roughly, ε_0 represents the strain at which the stress-strain relation changes from linear to exponential. Differentiating $W(\varepsilon_{ij})$ yields the associated elastic stress

$$\sigma_{ij}^{(e)} = \varepsilon_{ij}\left(\frac{\varepsilon_0}{\bar{\varepsilon}}\right)(e^{\bar{\varepsilon}/\varepsilon_0} - 1) \tag{7}$$

Note that for small strains where $\bar{\varepsilon} \to 0$, the elastic stress approaches the strain itself, that is, $\sigma_{ij}^{(e)} \to \varepsilon_{ij}$.

We turn now to a description of the cell stress. Based on the structure revealed by the micrographs in Fig. 1 we model the cells as slender rods of characteristic length l_0. By arbitrarily choosing one end of the cell to be "positive" and the other "negative," we can assign to the cell a direction in space, given by the unit vector n_i, as shown in Fig. 2 *a*. As

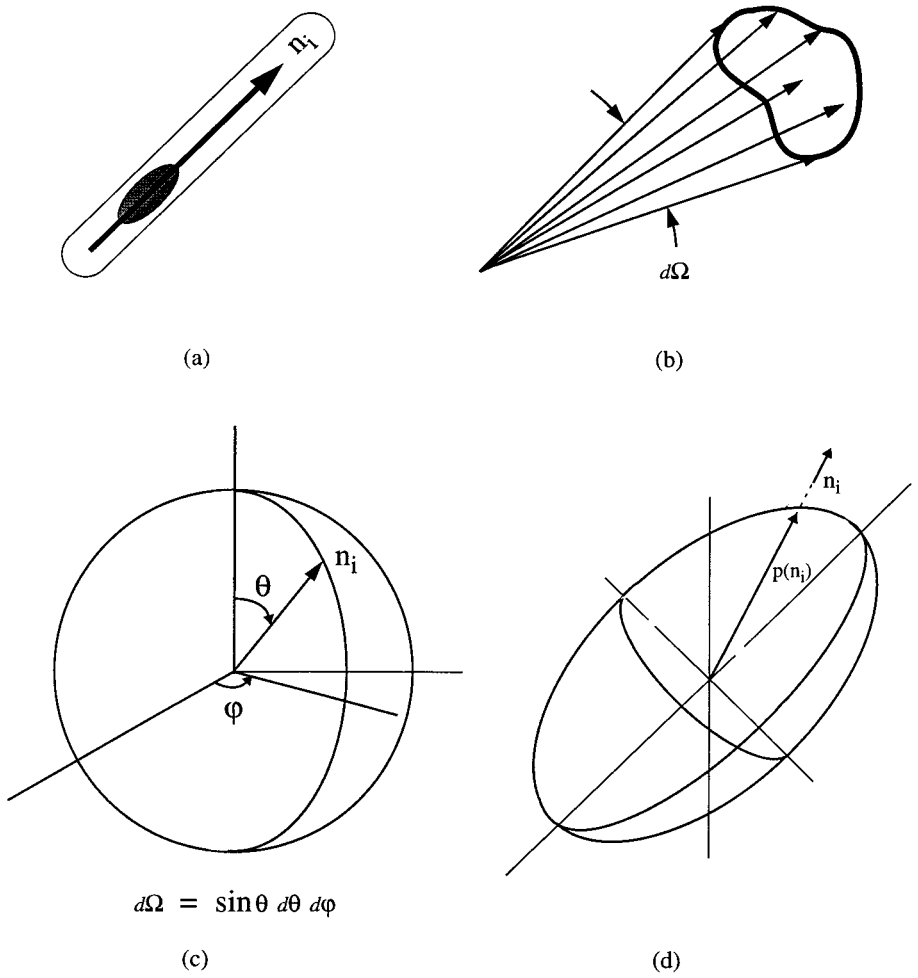

FIGURE 2 (*a*) The cell-orientation vector, n_i. (*b*) Solid angle, $d\Omega$, containing cell-orientation vectors. (*c*) Unit sphere, representing the distribution of cell-orientation vectors as points on its surface. (*d*) Closed surface representing the cell-orientation function, $p(n_i)$.

the cell direction varies from cell to cell, we can describe the distribution of directions by a cell orientation function, $p(n_i)$, with the property that within any elementary solid angle, $d\Omega$, about the direction n_i the fraction of the total cell population with directions within $d\Omega$ is given by $p(n_i)d\Omega$ (see Fig. 2 *b*). The distribution of cell orientations can also be described as points (the tips of the unit direction vectors) on a unit sphere. If an arbitrary coordinate system is selected with spherical polar angles θ and φ (Fig. 2 *c*) then $n_i(\theta, \varphi) = (\sin\theta\cos\varphi, \sin\theta\sin\varphi, \cos\theta)$ and $p(n_i)d\Omega = p(\theta, \varphi)\sin\theta\, d\theta\, d\varphi$. We expect that we can display the cell orientation function as a smooth closed surface of quasi-ellipsoidal shape, which is symmetric with respect to any line through the origin, as illustrated in Fig. 2 *d*; the distance from the origin to a point on this surface along a direction n_i is proportional to $p(n_i)$. As $p(n_i)$ is a probability-density function it must satisfy the normalization condition $\int p(n_i)d\Omega = 1$, where the integral extends over all directions. Two special cases are of particular interest. If the cell orientation is *isotropic*, then $p(n_i) = (1/4\pi)$, independent of cell direction, and is represented graphically as a sphere. If the cell orientation is *uniaxial* with direction $n_i^{(0)}$, then formally we may write $p(n_i) = \frac{1}{2}[\delta(n_i - n_i^{(0)}) + \delta(n_i + n_i^{(0)})]$, where δ is the Dirac function, and the graphical representation degenerates to a straight line along $n_i^{(0)}$.

Having modeled the geometrical character of the cells, we proceed to their mechanical properties. Cells, in particular fibroblasts, generate passive viscoelastic forces in response to deformation, as well as active contractile forces. As suggested by Fig. 3 *a* we consider the cells to be uniaxial contractile rods, producing a combination of active and passive force along their length. An arbitrary imaginary cutting plane will intersect some of these rods, and the forces they exert across this plane will determine, according to our assumptions, the cell stress, $\sigma_{ij}^{(c)}$. The problem of determining the contribution to the continuum stress of a distribution of contractile rods is one that is well known in theoretical polymer rheology (Bird et al., 1987), where it is shown that

$$\sigma_{ij}^{(c)} = Nl_0\langle Fn_in_j\rangle = Nl_0\int F(n_p)n_in_jp(n_q)d\Omega. \qquad (8)$$

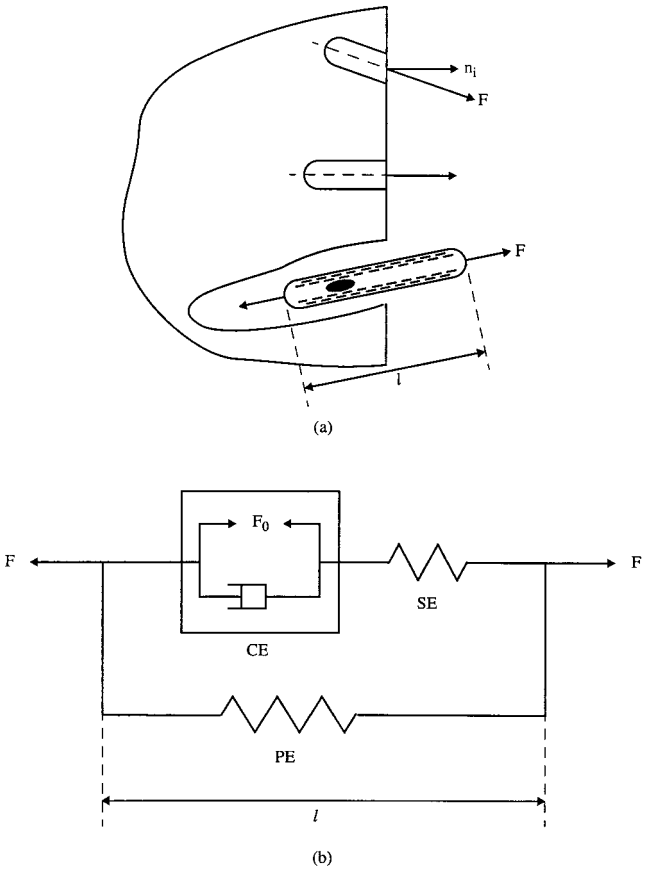

FIGURE 3 (*a*) Schematic diagram illustrating an imaginary cutting plane, with normal n_i, passing through matrix and cells. The cells generate a traction force F. (*b*) The classic Hill representation of a contractile rod of length l generating a force F. The model elements are: contractile force (F_0), contractile element (CE), series elastic element (SE), parallel elastic element (PE).

In the preceding equation F is the cell force, N is the number of cells per unit volume of tissue, l_0 is the cell length, and $\langle * \rangle = \int (*) p(n_i) d\Omega$ is the orientation-averaging operator.

For purposes of mechanical characterization we assume that an elongated cell is analogous to another well-studied biological linear force generator—namely, skeletal muscle. Indeed, it is likely that actin-myosin interactions contribute to the active force generated by the former, as by the latter. Following the work of A. V. Hill (1938) it has been traditional to represent the force generated by muscle as arising from a combination of three mechanical elements: a parallel elastic (PE) element accounting for the static passive mechanical properties, a series elastic (SE) element to account for the increased dynamic stiffness in activated cells, and finally a contractile element (CE) that embodies the active force-generating capabilities and quasi-viscous force-velocity response of the muscle. These three elements are shown in Fig. 3 *b*, and we assume that an elongated cell can be described by the same general mechanical paradigm.

For purposes of this initial development of a constitutive relation we will adapt a *linearized* version of the Hill model with constant parameters. Thus the force-velocity characteristic of the CE will be approximated by $\dot{l}_{CE} = (F_{CE} - F_0)/(\tau_c k_s)$, the force-length relation of the SE by $F_{SE} = k_s(l_{SE} - l_{SE0})$, and the force-length relation of the PE by $F_{PE} = k_p(l - l_0)$. Noting that $l = l_{CE} + l_{SE}$, $F_{CE} = F_{SE}$ and the total force $F = F_{SE} + F_{PE}$, these relations can be combined into a single ordinary differential equation governing the linearized mechanical behavior of a contractile rod.

$$\dot{F} + \frac{1}{\tau_c} F = \frac{1}{\tau_c} F_0 + l_0(k_s + k_p)\left(\frac{\dot{l}}{l_0}\right) + \frac{l_0 k_p}{\tau_c}\left(\frac{l}{l_0} - 1\right). \quad (9)$$

In the above equation F is the total force, l ($\approx l_0$) is the current cell length, k_s and k_p are respectively the series and parallel elastic stiffnesses of the cell, and τ_c is the cell time constant: the cell's effective viscosity, η_c, divided by k_s. The contractile force, F_0, represents the active force generated by the cell, and depends presumably on the concentration of some diffusible activator, such as bovine calf serum in our experiments. In the context of the traditional Hill muscle model, F_0 is usually referred to as the "isometric force" or the "active state."

To proceed from the constitutive equation for a single cell, Eq. 9, to an expression for the cell stress, we use two well-known results in continuum mechanics (Malvern). First, if a cell has direction n_i and the strain tensor is ε_{ij}, then the incremental stretch of the cell along its length is $(l/l_0) - 1 = (\Delta l/l_0) = \varepsilon_{ij} n_i n_j$. Clearly the cell stretch depends on the cell direction. Second, the fractional rate of change of cell length ($\dot{l}/l$) is related to the rate-of-deformation tensor, $d_{ij} = \frac{1}{2}(v_{i,j} + v_{j,i})$, as $(\dot{l}/l) = d_{ij} n_i n_j$; v_i is the tissue velocity. Because we are assuming small strains, we may approximate $(\dot{l}/l) \approx (\dot{l}/l_0)$ and $d_{ij} \approx \dot{\varepsilon}_{ij} = (\partial \varepsilon_{ij}/\partial t)$, and obtain $(\dot{l}/l_0) \approx \dot{\varepsilon}_{ij} n_i n_j$. Again, the cell's strain rate depends on direction. It is important to recognize that both of these conclusions are based on the assumption that the cells follow the macroscopic deformation of the tissue continuum (See Discussion.)

The remaining steps are purely mechanical. First we multiply both sides of the cell constitutive equation, Eq. 9, by $N l_0 n_p n_q p(n_k) d\Omega$ and integrate over all directions, that is,

$$N l_0 \int \left\{ \dot{F} + \frac{1}{\tau_c} F \right\} n_p n_q p(n_k) d\Omega$$

$$= N l_0 \int \left\{ \frac{1}{\tau_c} F_0 + l_0(k_s + k_p)\dot{\varepsilon}_{ij} n_i n_j + \frac{l_0 k_p}{\tau_c} \varepsilon_{ij} n_i n_j \right\} n_p n_q p(n_k) d\Omega \quad (10)$$

In view of Eq. 8 this yields

$$\frac{\partial \sigma_{pq}^{(c)}}{\partial t} + \frac{1}{\tau_c}\sigma_{pq}^{(c)} = \frac{3}{\tau_c}\sigma_0 A_{pq} + \left(\kappa\frac{\partial}{\partial t} + \frac{\omega}{\tau_c}\right)(B_{pqij}\varepsilon_{ij}) \qquad (11)$$

as the constitutive equation for the cell stress, where the macroscopic tissue parameters appearing in Eq. 11 are related to the individual cell parameters by

$$\sigma_0 = \tfrac{1}{3}Nl_0F_0, \quad \kappa = Nl_0^2(k_s + k_p), \quad \omega = Nl_0^2k_p. \qquad (12)$$

In deriving Eq. 11 it was assumed that the contractile force F_0 is independent of cell orientation. The parameter σ_0 may be dubbed the cell "contractile pressure," although it actually represents an isotropic tension if it is positive. The parameter ω represents the macroscopic manifestation of cellular parallel elasticity, and κ the combination of parallel and series elasticity. Two tensors, A_{ij} and B_{ijpq}, appeared in the derivation of Eq. 11, and we designate these as the "cell anisotropy tensors." They are defined as

$$A_{ij} = \langle n_i n_j \rangle = \int n_i n_j p(n_k) d\Omega \qquad (13)$$

and

$$B_{ijpq} = \langle n_i n_j n_p n_q \rangle = \int n_i n_j n_p n_q p(n_k) d\Omega \qquad (14)$$

The appearance of these two tensors in Eq. 11 translates the anisotropy of the microscopic cell distribution into anisotropic mechanical behavior of the macroscopic tissue.

We have now arrived at our final result, in which we combine the cell constitutive equation, Eq. 11, with the matrix constitutive equation, Eq. 3, via Eq. 1, to obtain a constitutive equation for the tissue (FPM). For consistency with Eq. 3 we also convert Eq. 11 to integral form, obtaining

$$\sigma_{ij} = \int_{-\infty}^{t}\left[\lambda(t-\hat{t})\delta_{ij}\left(\frac{\partial \sigma_{kk}^{(e)}}{\partial \hat{t}}\right) + 2\mu(t-\hat{t})\left(\frac{\partial \sigma_{ij}^{(e)}}{\partial \hat{t}}\right) + e^{-(t-\hat{t})/\tau_c}\left\{\frac{3}{\tau_c}\sigma_0 A_{ij} + \left(\kappa\frac{\partial}{\partial \hat{t}} + \frac{\omega}{\tau_c}\right)(B_{ijpq}\varepsilon_{pq})\right\}\right] d\hat{t}. \qquad (15)$$

For incompressible materials the first term on the right side of Eq. 15, $\int \lambda(t-\hat{t})\delta_{ij}(\partial \sigma_{kk}^{(e)}/\partial \hat{t})d\hat{t}$, is simply replaced by $-p\delta_{ij}$. A qualitative spring-dashpot representation of the (incompressible) material described by Eq. 15 is presented in Fig. 4, and should provide an intuitive sense of its mechanical behavior.

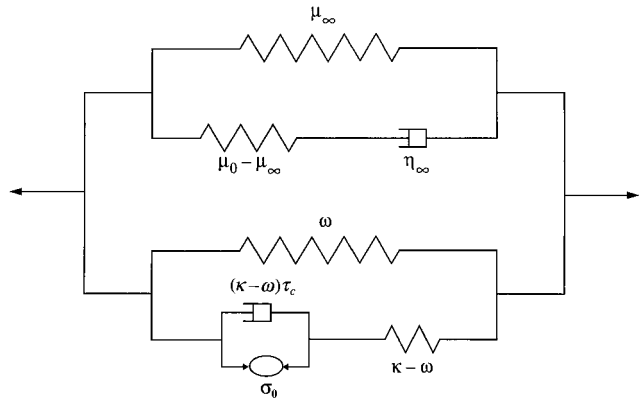

FIGURE 4 Spring-dashpot representation of the tissue model constitutive relation, Eq. 15. This representation is only qualitative because 1) the matrix portion of the constitutive relation is, in general, nonlinear, and 2) the cell portion of the constitutive relation is, in general, anisotropic. The figure becomes quantitatively accurate in the special case of a matrix composed of linear standard-solid material, together with a uniaxial cell orientation.

THE CELL ANISOTROPY TENSORS A_{ij} AND B_{ijpq}

The second-rank tensor A_{ij} and the fourth-rank tensor B_{ijpq} are important because they connect the distribution of cell orientations, which is determined by the fabrication conditions, to the macroscopic mechanical behavior of the FPM. These tensors are completely determined by the cell orientation function, $p(n_i)$, which must be measured experimentally. For reference, we list some of their salient properties, which may be verified by the definitions given in Eqs. 13 and 14.

1. The components of A_{ij} and B_{ijpq} are at most one in absolute value;
2. A_{ij} and B_{ijpq} are symmetric with respect to any pair of indices;
3. $B_{ijkk} = A_{ij}$;
4. There are at most six independent components of A_{ij} and 15 independent components of B_{ijpq};
5. For a planar distribution, where one component of n_i is equal to zero, there are at most three independent nonzero components of A_{ij} and five independent nonzero components of B_{ijpq};
6. For a uniaxial cell distribution in the 1-direction all components of A_{ij} and B_{ijpq} are zero except $A_{11} = 1$ and $B_{1111} = 1$;
7. For three-dimensional isotropy

$$A_{ij} = \tfrac{1}{3}\delta_{ij}$$

and

$$B_{ijpq} = \tfrac{1}{15}(\delta_{ij}\delta_{pq} + \delta_{ip}\delta_{jq} + \delta_{iq}\delta_{jp}), \quad \text{where } i, j = 1, 2, 3;$$

8. For planar isotropy (isotropy in the 1-2 plane, with $n_3 = 0$) all components that contain 3 as an index vanish, and

$$A_{\alpha\beta} = \tfrac{1}{2}\delta_{\alpha\beta}$$

and

$$B_{\alpha\beta\gamma\rho} = \tfrac{1}{8}(\delta_{\alpha\beta}\delta_{\gamma\rho} + \delta_{\alpha\gamma}\delta_{\beta\rho} + \delta_{\alpha\rho}\delta_{\beta\gamma}), \quad \text{for } \alpha, \beta = 1, 2.$$

Except in the degenerate cases of uniaxial, isotropic, and planar isotropic distributions the anisotropy tensors must be computed using the measured cell orientation function, $p(n_i)$.

ANALYSIS OF RELAXATION

Using Eq. 15 we can compute the tissue response in a relaxation test, which we will compare to measured relaxation responses in the next section. In this analysis we will make several approximations which our experimental observations suggest are acceptable to first-order. First, we assume that the matrix is incompressible. Next, we suppose that when the cell forces have been eliminated by application of appropriate drugs (high concentrations of cytochalasin D, in our experiments) then this implies that $\sigma_0 = \kappa = \omega = 0$. Then Eq. 15 reduces to the following constitutive equation for the passive matrix

$$\sigma_{ij} = -p\delta_{ij} + 2\int_{-\infty}^{t} \mu(t - \hat{t})d\sigma_{ij}^{(e)} \tag{16}$$

The test specimen of initially unstrained tissue, from which cell contributions have been eliminated with cytochalasin D, is subjected to a homogeneous step of uniaxial strain ε_{11} at $t = 0$, which is subsequently held constant. As the matrix has been assumed incompressible and isotropic, there will be concurrent lateral strains $\varepsilon_{22} = \varepsilon_{33} = -(\varepsilon_{11}/2)$. According to Eq. 16 the stress response to the strain step is

$$\sigma_{ij} = -p\delta_{ij} + 2\mu(t)\sigma_{ij}^{(e)}(\varepsilon_{pq}) \tag{17}$$

or

$$\sigma_{11} = -p + 2\mu(t)\sigma_{11}^{(e)}$$

and (18)

$$\sigma_{22} = -p + 2\mu(t)\sigma_{22}^{(e)} = 0$$

The pressure, p, can be determined from the second of Eqs. 18, and when inserted into the first yields

$$\sigma_{11}(t) = 2\mu(t)[\sigma_{11}^{(e)} - \sigma_{22}^{(e)}] \tag{19}$$

$\sigma_{ij}^{(e)}$ is given as a function of ε_{ij} by Eq. 7. It is easy to show that in a uniaxial strain of an incompressible material $\bar{\varepsilon} = \varepsilon_{11}$, so that Eq. 19 becomes

$$\sigma_{11}(t) = 3\mu(t)\varepsilon_0(e^{\varepsilon_{11}/\varepsilon_0} - 1). \tag{20}$$

Comparing Eq. 20 to uniaxial relaxation stresses $\sigma_{11}(t)$, measured in cytochalasin D-treated FPMs for several constant values of the uniaxial strain, it is possible to identify the parameter ε_0 and the relaxation function, $\mu(t)$. We denote the special values $\mu(0) = \mu_0$ (the "fast" stiffness), $\mu(\infty) = \mu_\infty$ (the "slow" stiffness), and $\eta_\infty = \int_0^\infty[\mu(t) - \mu(\infty)]dt$, the matrix steady-state viscosity, by the indicated symbols.

The above analysis holds for substantial strain amplitudes where the stress is a nonlinear function of the strain, but due to technical constraints the relaxation tests described in the next section were limited to strains of <0.06. As experimental measurements suggest that $\varepsilon_0 \approx 0.1$, under these circumstances it is reasonable to make the approximation that $\sigma_{ij}^{(e)}(\varepsilon_{pq}) \doteq \varepsilon_{ij}$. This greatly simplifies the subsequent analysis of the active tissue response, so for the remainder of this section we will adopt this linearization of the "elastic" stress $\sigma_{ij}^{(e)}$ and set it equal to the strain. Then Eq. 20 becomes

$$\sigma_{11}(t) = 3\mu(t)\varepsilon_{11} \tag{22}$$

which gives the matrix relaxation function, $\mu(t)$, directly in terms of the observed variation of the passive stress, $\sigma_{11}(t)$ for constant strain step ε_{11}.

We turn now to the relaxation response with the cells active. For purposes of this analysis we assume that the cell distribution is planar isotropic. Under these circumstances $A_{\alpha\beta} = \frac{1}{2}\delta_{\alpha\beta}$ and $B_{\alpha\beta\gamma\rho}\varepsilon_{\gamma\rho} = \frac{1}{8}(\varepsilon_{\gamma\gamma}\delta_{\alpha\beta} + 2\varepsilon_{\alpha\beta})$ with $\alpha, \beta, \gamma, \rho = 1,2$ and all other components are zero. If the cells are activated at a remote time prior to $t = 0$ by holding constant the concentration of a diffusible chemical stimulant, with $\varepsilon_{11} = 0$, it is easy to show using Eq. 15 and the conditions of incompressibility ($\varepsilon_{11} + \varepsilon_{22} + \varepsilon_{33} = 0$) and uniaxial stress ($\sigma_{22} = \sigma_{33} = 0$) that the tissue will have attained a constant steady state at $t = 0^-$, with the values

$$\varepsilon_{22}(0^-) = -\left(\frac{12}{3\omega + 32\mu_\infty}\right)\sigma_0$$

and (22)

$$\sigma_{11}(0^-) = \tfrac{3}{2}\left(\frac{2\omega + 16\mu_\infty}{3\omega + 32\mu_\infty}\right)\sigma_0$$

where σ_0 is the constant cell pressure, a measure of activation level. If now a uniaxial strain step $\Delta\varepsilon_{11}$ is imposed at $t = 0$ while maintaining the cell pressure (i.e., activation), σ_0, constant, this will give rise to transverse strain increments, $\Delta\varepsilon_{22}$ and $\Delta\varepsilon_{33}$, as well as an axial stress increment $\Delta\sigma_{11}(t)$. Again using Eq. 15, with $\sigma_{ij}^{(e)} = \varepsilon_{ij}$, and the auxiliary conditions $\Delta\varepsilon_{11} + \Delta\varepsilon_{22} + \Delta\varepsilon_{33} = 0$ and $\Delta\sigma_{22} =$

$\Delta\sigma_{33} = 0$, it can be shown after some calculation that

$$\left(\frac{\Delta\sigma_{11}}{\Delta\varepsilon_{11}}\right) = \frac{1}{8}\frac{[2\upsilon(t) + 16\mu(t)][4\upsilon(t) + 48\mu(t)]}{[3\upsilon(t) + 32\mu(t)]} \quad (23)$$

where

$$\upsilon(t) = \omega + (\kappa - \omega)e^{-t/\tau_c} \quad (24)$$

If we define, for algebraic convenience, $x = [(\Delta\sigma_{11}/3\mu\Delta\varepsilon_{11}) - 1]$ and $y = \upsilon/\mu$, then Eq. 23 may be written as $3x(32 + 3y) = y(11 + y)$, which may be solved for y in terms of x, yielding

$$y = \tfrac{1}{2}\{\sqrt{81x^2 + 186x + 121} + 9x - 11\} = 9x + \xi. \quad (25)$$

It can be shown that the error, ξ, of approximating y by $9x$ is $<3\%$ for all positive x. Ignoring this small error and assuming that $y = 9x$, we obtain the simple result that

$$\upsilon = 3[(\Delta\sigma_{11}/\Delta\varepsilon_{11}) - 3\mu]$$

or

$$\omega + (\kappa - \omega)e^{-t/\tau_c} = 3\left[\frac{\Delta\sigma_{11}}{\Delta\varepsilon_{11}} - 3\mu\right]. \quad (26)$$

The function $3\mu(t)$ is simply the *passive* response (i.e., relaxation function) with cell forces absent, so Eq. 26 states that the *difference* between the total and passive relaxation responses can be interpreted directly in terms of cellular mechanical properties. As $\kappa > \omega > 0$, this difference is predicted to be a decaying function of time—a typical relaxation function; indeed, this function is predicted to be a *monoexponential* function by this initial version of our theory. Equations 22 and 26 are used in the next section to extract cell-mechanical parameters from our measurements of relaxation responses. Note that by integrating Eq. 26 one can extract a measure of cell viscosity

$$\eta = (\kappa - \omega)\tau_c = \int_0^\infty \left[3\left\{\frac{\Delta\sigma_{11}}{\Delta\varepsilon_{11}} - 3\mu\right\} - \omega\right]dt; \quad (27)$$

the viscosity per cell is $\eta_c = \eta/(Nl_0^2)$.

RELAXATION EXPERIMENTS

Sample preparation and mechanical measurements

Detailed methods can be found elsewhere (Wakatsuki et al., 2000). Briefly, 1.0×10^6 chicken embryo fibroblasts (CEFs) were re-suspended in 1 ml DMEM containing 10% FBS and 1 mg rat tail collagen (Upstate Biotechnology, Lake Placid, NY). The cell-collagen mixed solution was poured into cylindrical wells with a central mandrel and placed in the tissue culture incubator (5% CO_2 and 37°C) for 2 days (with FBS absent during the last 16 h). An FPM ring formed around the mandrel and was gently removed for subsequent testing. After incubation and compaction the water content of the extracellular matrix was 99%. The FPM rings were looped over a stainless steel hook attached to an isometric force transducer and over a horizontal rod attached to a stepper motor. The distance between the lower rod and the hook was set at half the circumference of the mandrel, thereby restoring the FPM to its original length (0% strain). The motor was controlled by custom software (developed by Bill McConnaughey) running on a personal computer.

Reagents

Cytochalasin D (Sigma, St. Louis, MO) was dissolved in dimethyl sulfoxide (DMSO) at a concentration of 2 mM as a stock solution. This stock solution was added to the tissue culture medium in an organ bath at 1/1000 dilution.

Cell orientation measurements

The cells in the FPMs were stained with the cytoplasmic fluorescent dye Cell Tracker (Molecular Probes, Eugene, OR) for 15 min in the incubator. The samples were then washed twice with phosphate buffered saline (PBS) to remove excess dye, and fixed with 3.7% formaldehyde in PBS for 30 min at room temperature. The confocal images of fluorescently labeled CEFs were taken as 36 sections at 2 μm intervals of the tissue normal to its thickness. Almost all the spread cells exhibited bipolar spindle shapes. To determine the directions of the long axes of bipolar spindle-shaped cells, each image was analyzed using a macro program written for ScionImage software (Scion Corp., Frederick, MD). The cells that were round or too close to other cells were simply ignored in the analysis.

RESULTS

Cell orientation

The fibroblasts spread in bipolar spindle shapes ($\sim$100 μm length and $\sim$50 μm^2 cross-sectional area at nuclei) in the FPM, and were visualized using cytoplasmic fluorescent dye. Sections of confocal images at the center and near the free edge of the FPM are shown in Fig. 1, *A* and *B*, respectively. The cells near the edge were oriented parallel to the edge, whereas the cells at the center were oriented almost in random directions. In both locations the cells were densely packed and often made contact with each other. This suggests the existence of an almost continuous cell network throughout the FPMs. To determine the cell-orientation distribution we measured the angle between the long axis of a cell and the circumferential direction of the ring (parallel to the uniaxial stretch direction). A polar plot of the cell-orientation distribution shows the number of cells ori-

TABLE 1 Active: cell parameters estimated from relaxation tests

Strain	Force (dyne) ($t = 0$)	Force (dyne) ($t \to \infty$)	κ (dyne/mm^2)	ω (dyne/mm^2)	τ_c (s)
0.01	140.8 ± 50.5	12.3 ± 15.7	10,560 ± 3788	923 ± 1178	1.38
0.02	136.1 ± 30.1	26.5 ± 6.4	5104 ± 1129	994 ± 240	1.98
0.04	195.8 ± 97.7	33.8 ± 14.4	3671 ± 1832	634 ± 270	0.72
0.06	249.6 ± 40.3	35.1 ± 9.5	3120 ± 504	439 ± 118	0.96
		Average:	5164	748	1.26

ented within a fixed angular interval (10°) as a function of the angle at the center of the interval (Fig. 1 *C*). The FPMs made with low cell concentrations (100,000 cells/ml, initial) exhibited sparsely distributed and randomly oriented cells in almost the entire sample (Fig. 1 *D*).

Stress relaxation

The FPMs were first stretched using a stretch cycle of 20% strain (15 min each of elongation and shortening at steady rate), which preconditions the sample (Wakatsuki et al., 2000). When the force reached a steady level after the preconditioning cycle, the FPMs were subjected to a fast step stretch within 0.1 s. The strain of the FPMs was kept constant for at least 30 min to observe the force relaxation down to a steady level, and the recorded force versus time curve is called the "Total" response. After the end of the relaxation the strain was returned to 0% and the sample was permitted to recover to its initial state. After recovery, 2 μM cytochalasin D was added to disrupt the actin filaments, which presumably abolishes the cellular contribution to the tissue force. After the force reached a new steady-state value (normally very small, practically zero), another rapid step stretch was applied and the force relaxation was recorded at least for 30 min, and called the "Passive" response. This stress relaxation curve, after cytochalasin D treatment, is interpreted as representing the passive matrix properties, and is analyzed using Eq. 21. The stress-relaxation curve obtained by subtracting the Passive curve from the Total curve is called the "Active" response; it is associated with the cellular contribution to tissue mechanics, and is analyzed using Eq. 26.

Steps of several amplitudes (0.01, 0.02, 0.04, and 0.06) strain were applied to the samples. The step force, which is the difference between the peak force (at $t = 0^+$) and the steady initial force (at $t = 0^-$), was measured from both the Passive and Active curves, and the values are listed in Tables 1 and 2. The steady force after stress relaxation (as $t \to \infty$) obtained from the Active (Table 1) and Passive (Table 2) curves, for several strain levels, are also shown in Tables 1 and 2. Both the step force and the relaxed force are listed as mean ± SD over repeated trials under nominally identical conditions, so the standard deviation is a measure of the experimental reproducibility of the force. Our theory predicts that the tabulated Passive and Active forces should vary linearly (indeed, proportionately) with the strain. Linear regressions relating the strain to the Passive force at $t = 0$, the Passive force at $t = \infty$, the Active force at $t = 0$, and the Active force at $t = \infty$ produced correlation coefficients of 0.99, 0.98, 0.91, and 0.90, respectively; these correlations included the origin as a measured data point. As a measure of the proportionality between force and strain we may list the ratio of the absolute force predicted by the linear regression at the maximum strain (0.06) to that predicted at zero strain; for the four cases listed above these ratios were 15.1, 162, 5.0, and 5.1. We accept this as adequate confirmation of linearity for the present, subject to future verification by more extensive measurements. Clearly, the measured deviations from proportionality between force and strain are greater for the Active force than for the Passive, suggesting that the cell stiffness parameters may vary somewhat with strain. To assign definite values to the matrix (μ_0, μ_∞) and cell (κ, ω) stiffness moduli the values were averaged over all measured strain levels, and are listed in Tables 1 and 2. Note that as the force was the only measured quantity assumed to exhibit statistical variability in the calculation of these moduli, the (standard deviation/mean) ratios of the moduli are the same as those of the corresponding forces. The matrix and cell relaxation times were measured as the half-times, $t_{1/2}$, of the relaxation curves, and converted to equivalent monoexponential relaxation times by the relation τ_m, $\tau_c = t_{1/2}/\ln 2$; values of the order of one second were observed at all strain levels and are listed in Tables 1 and 2. The relaxation properties of the passive matrix are charac-

TABLE 2 Passive: matrix parameters estimated from relaxation tests

Strain	Force (dyne) ($t = 0$)	Force (dyne) ($t \to \infty$)	$3\mu_0$ (dyne/mm^2)	$3\mu_\infty$ (dyne/mm^2)	τ_m (s)
0.01	35.1 ± 7.6	23.7 ± 4.4	878 ± 190	593 ± 110	1.38
0.02	43.1 ± 18.5	28.4 ± 12.8	539 ± 231	355 ± 160	1.14
0.04	145.0 ± 27.5	58.05 ± 11.9	907 ± 172	363 ± 74	3.96
0.06	261.3 ± 3.3	101.9 ± 5.3	1089 ± 14	425 ± 22	3.78
		Average:	853	434	2.57

TABLE 3 Additional parameters

Parameter	Value
Cell contractile stress, σ_0	421 Pa
FPM cross-sectional area, A_t	4 mm^2
FPM length	15 mm
Cell density, N	16,700 cells/mm^3
Cell length, l_0	0.1 mm
Cell cross-sectional area, A_c	5×10^{-5} mm^2
$A_t \cdot \sigma_{11}$ (0^-)	140.5 $\pm$ 18.1 dyne ($n = 4$)

terized graphically by its relaxation function (the passive curve in Fig. 5). In this preliminary analysis we have characterized each relaxation curve by a single matrix or cell time constant. As noted, this dominant time constant is small (seconds), but Fig. 5 shows clearly that the relaxation responses also contain slow components with much larger time constants (minutes); these may be important for slow deformations, and will be analyzed in more detail in future work. Additional parameters are listed in Table 3, including the average steady pre-step tension $A_t \cdot \sigma_{11}(0^-)$. The final cell concentration, N, in the compacted tissue is estimated from the initial cell concentration and the change in volume, measured by the methods explained previously (Wakatsuki et al., 2000). We assumed no significant change in cell number.

DISCUSSION

The primary objective of the constitutive theory developed in this paper is to provide a mathematical basis from which one can interpret the mechanical behavior of whole tissue in terms of the mechanical properties of its matrix and cellular constituents. It is a first attempt which can be, and almost certainly will be, elaborated and improved as our experimental and theoretical experience grows. But even in its present form we believe that the theory provides a useful tool for understanding the mechanics of cell-matrix tissue composites. To develop a tractable constitutive relation we have made several assumptions, including the following:

1. *The formed tissue is stable.* Thus we do not consider the possible migration of cells within the matrix, or the internal remodeling of cells in response to mechanical stresses. Our experimental observations indicate that this is an acceptable assumption, at least on the time scale of our measurements.

2. *The small-strain tensor is adequate to describe the tissue deformation.* In this first iteration of our theory we wish to avoid the additional complexity of nonlinear deformation kinematics. Our experiments extend to ~20% strain, and at that limit the small-strain assumption becomes questionable, but the inherent error does not seem out of line with that of our other assumptions.

3. *The tissue stress is the sum of a matrix stress and a cell stress.* We interpret this assumption in a strict sense to mean that the matrix stress is the stress generated in the matrix in the absence of cell force and the cell stress is the actual force per unit area of imaginary cutting plane exerted by the cells cut by the plane. Under this interpretation there is no theoretical reason why this assumption should be strictly true, and indeed it is not true in general. Nevertheless, an additive stress decomposition has been assumed in all previously published theories of tissue mechanics (Murray et al., 1983; Murray and Oster, 1984; Tranquillo and Murray, 1992), as well as in other fields such as muscle mechanics and polymer rheology, so we tentatively adopt it here as an acceptable approximation subject to future verification studies.

4. *The cells deform with the continuum.* Again, this is an approximation for which there is no theoretical necessity. The ratio of the linear strain of a cell along its length to the macrostrain of the tissue in which it is embedded is a complicated function of the stiffnesses and viscosities of both the cells and the matrix, the cell dimensions, and the cell concentration. For the values of cell and matrix properties deduced from our relaxation tests, listed in Tables 1–5, simple order-of-magnitude calculations suggest that the cell strain should indeed be close to the tissue strain. Furthermore, at the higher cell concentrations encountered

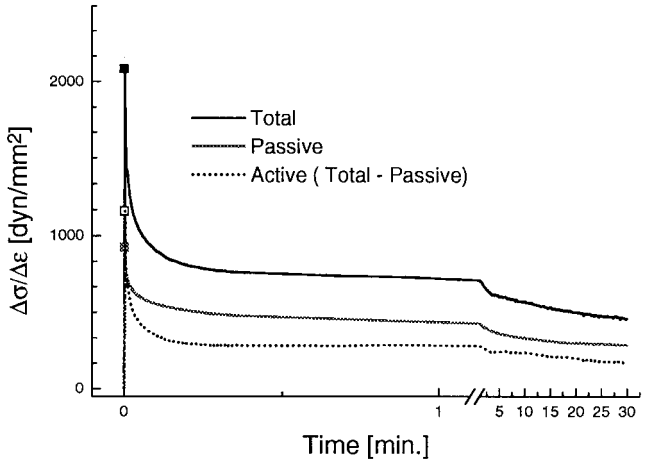

FIGURE 5 Experimental relaxation curves (see Tables 1–3 for parameters). The Total curve was measured before, and the Passive curve was measured after, treatment with cytochalasin D. The Active curve is the difference between the Total and Passive curves. Note the change in time scale on the horizontal axis.

TABLE 4 Single-cell parameters estimated by our model

Cell Parameter	Value
Cell force, F_0	756 nN
Parallel stiffness, k_p	4.5 dyne/mm ($\rightarrow$ 0.09 MPa*)
Series stiffness, k_s	29.1 dyne/mm ($\rightarrow$ 0.583 MPa*)
Cell viscosity, η_c	36.7 dyne-s/mm ($\rightarrow$ 0.245 MPa-s*)

*Equivalent continuum moduli for homogeneous rod with fibroblast dimensions (see text).

TABLE 5 Single-cell parameters estimated from previous publications

Cell Parameter	Cell Type	Value	Reference
Cell force	Human small artery	0.1–2 nN	Intengan et al. (1999)
	Leukocyte*	0.8 nN	Evans and Young (1989)
	Fibroblast	500 nN	Kolodney and Wysolmerski (1992)
	Fibroblast	1000 nN	Wakatsuki et al. (2000)
	Active skeletal muscle†	12,500 nN	Ford et al. (1981)
Elastic modulus	Leukocyte (k_p, k_s)	(1.1, 36) Pa	Sung et al. (1988)
	Leukocyte	0.3–0.9 kPa	Zahalak et al. (1990)
	Fibroblast (cortex)	0.06–0.12 MPa	Bausch et al. (1999)
	Single smooth muscle	1.2 MPa	Glerum et al. (1990)
	Fibroblast	2.5 MPa	Wakatsuki et al. (2000)
	Active skeletal muscle‡	20 MPa	Ford et al. (1981)
Cell viscosity	Leukocyte	33 Pa-s	Sung et al. (1988)
	Leukocyte	200 Pa-s	Evans and Young (1989)
	Fibroblast	200 Pa-s	Bausch et al. (1999)
	Active skeletal muscle§	0.26 MPa-s	Katz (1939)

*Estimated from cortical tension.
†With dimensions of a fibroblast.
‡Estimated from T_2 response.
§Estimated from force-velocity relation in stretch.

in our tissue models, the cells appear close to forming an interconnected net, and under these circumstances the assumption does not seem unreasonable. The same sort of assumption is made, for example, in the theory of rubber hyperelasticity (Wall, 1958). In future work we intend to examine this assumption more closely via both experimental and computational approaches.

5. *The cells are identical thin contractile rods.* We believe that our observations of spread cells in formed tissue, as illustrated in Fig. 1, justify this geometrical approximation about the shape of the rods. This allows us to define and measure a cell orientation function. Obviously the cells are not all identical, but our assumption that they are (except for orientation) seems to us an acceptable "pre-averaging" to facilitate the construction of this initial theory.

6. *The cells can be characterized mechanically by a Hill muscle model.* While fibroblasts and other nonmuscle cells lack long-range ordered sarcomeric structure, they share with muscle cells an ability to generate active contractile force, probably based also on actin-myosin interactions (Kolodney and Elson, 1993). Furthermore, mechanical measurements (using micropipettes, the cell poker, and other techniques) on isolated cells have shown clearly that they exhibit viscoelastic behavior. The minimum number of parameters needed to describe such behavior is three: a "fast" elasticity, a "slow" elasticity, and a viscosity. The Hill model provides these three parameters through its "series" elasticity, "parallel" elasticity, and "force-velocity" relation. The linearization of the Hill model was adopted at this initial stage of model development for mathematical convenience, and it greatly simplifies model development and interpretation.

Most of these assumptions can be relaxed if one is willing to pay the price in model complexity. For example, it seems feasible, following Barocas and Tranquillo (1997), to postulate a connection between the cell orientation $p(n_i)$, and the tissue strain. Terms of higher order than the first (i.e., the small-strain tensor) could be retained in an expansion of the Green strain, in an attempt to characterize deformation kinematics more accurately. Experimental measurements of actual individual cell deformations, as well as finite-element studies, may suggest more appropriate relations between the tissue macrostrain and individual cell deformation. The cell mechanical properties could be characterized by relations more sophisticated than the linearized Hill model that we used. For example, if the uniaxial passive response of an individual cell is characterized by a general linear viscoelastic relation of the form $F = \int_{-\infty}^{t} G(t - \hat{t})\dot{l}\, d\hat{t}$, then in averaging over cell orientation this will contribute a term $\sigma_{ij} = \int_{-\infty}^{t}\{Nl_0^2 G(t - \hat{t})\}B_{ijpq}\dot{\varepsilon}_{pq}d\hat{t}$ to the tissue constitutive relation; thus $Nl_0^2 G(t)B_{ijpq}$ appears as the (in general, anisotropic) macroscopic tissue relaxation function associated with the embedded cells. These refinements of the basic theory and others we reserve for future work. In this initial report we concentrate on a description of a path by which one can proceed from cell and matrix properties to composite tissue properties and first-order estimates of the model parameter values.

The limited experimental data that we have presented seems to provide support for the theory, at least as a first approximation of the mechanics of cell-matrix interaction. As the initial version of our theory assumes constant values for the cell stiffness and viscosity parameters, it predicts that the difference between the measured Total and Passive curves should be a monoexponentially decaying function (Eq. 26). Fig. 5 confirms that the Active relaxation curve is indeed monotonically decreasing and can be fit fairly well by a monoexponential decay—although, not surprisingly, a

bi-exponential provides a better fit. This result is significant, because the mere fact that the Total and Active curves are monotonically decreasing does ensure that their difference will also decrease monotonically, as observed and required by the theory. More detailed modeling of the relaxation characteristics of individual cells, and more careful accounting for the actual orientation distribution of the cells (planar isotropic in the central region and uniaxial near the edges) may reduce the differences between the measured and predicted Active curves.

The analysis of relaxation presented in the Theory section of this paper assumes that the matrix is an incompressible material. We have partially confirmed this assumption by simultaneously measuring the axial and transverse strain in the planes perpendicular to the thickness direction of cytochalasin D-treated FPMs. This was done by measuring the movement of small embedded markers; the ratio of transverse strain to axial strain was found to be close to 0.5, which is consistent with the assumption of isotropy. A full confirmation of material isotropy will require simultaneous measurement of axial strain, transverse strain in the plane of the sample, and transverse strain perpendicular to the plane of the sample (i.e., in the thickness direction). These measurements are technically difficult, but we will attempt them in the future.

An examination of the cell stiffness moduli and matrix stiffness moduli in Tables 1 and 2 reveals that the cellular contribution to the tissue stiffness is comparable to that of the matrix. This is because a planar isotropic cell orientation introduces a factor of (1/8) into the term $B_{ijpq}\varepsilon_{pq}$ (see discussion of the cell-anisotropy tensors), so that κ and ω should each be divided by 8 before comparing them with the passive relaxation moduli $2\mu_0$ and $2\mu_\infty$, respectively; thus $(\kappa/8)/2\mu_0 = 1.23$ and $(\omega/8)/2\mu_\infty = 0.32$. A similar conclusion can be reached by comparing the active and passive uniaxial response, according to Eq. 26, where $[\kappa/3]/(3\mu_0) = 2.19$ and $[\omega/3]/(3\mu_\infty) = 0.57$. Thus it appears that the cell contribution to the total tissue stiffness is somewhat higher relative to the matrix contribution in fast loading than in slow loading, but neither clearly dominates. The relative contribution of the matrix may increase still further over time due to continued deposition and cross-linking of the matrix proteins.

Values of individual cell parameters, calculated from the moduli listed in Table 1 via Eqs. 12 and 22, and the viscosity relation $\eta_c = k_s\tau_c$, are listed in Table 4. For comparison, some cell parameter estimates based on previously published reports are listed in Table 5. We calculate the force produced by a single fibroblast to be 756 nN, which is close to that estimated from a previous analysis using the measured cell cross-sectional areas of FPMs (Kolodney and Wysolmerski, 1992; Wakatsuki et al., 2000; Table 5). It is also close to the cell force produced by a single smooth muscle cell (Harris and Warshaw, 1991). This force, however, is much larger than that deduced from the cortical surface tension in isolated leukocytes, 0.8 nN (Evans and Young, 1989). The (fast) elastic modulus of the fibroblast is estimated, from the sum of k_s and k_p, to be 0.67 MPa, which approaches a previous estimate for fibroblasts in a collagen matrix listed in Table 5, measured by oscillatory length perturbations (Wakatsuki et al., 2000) and that of single smooth muscle cells (Glerum et al., 1990). (For the purpose of comparing our theoretical parameter estimates for a single fibroblast to those published previously in the literature, we have viewed the cell as a homogeneous, incompressible rod and calculated equivalent Young's moduli, E, and viscosity modulus, D, according to $(E_s, E_p) = (k_s, k_p)(l_0/A_c)$ and $D = \eta_c(l_0/3A_c)$, where l_0 (=0.1 mm) is the cell length and A_c (=50 μm^2) is the cell cross-sectional area. These moduli are listed in parentheses in Table 4.) The similarities in the magnitudes of cell parameters to those of smooth muscle cells could be due to the phenotypic change often observed in the fibroblasts in granulation tissue (Darby et al., 1990). These fibroblasts, usually dubbed "myofibroblasts," express α-smooth muscle actin, presumably to produce higher tension for wound closure. The estimate of Bausch et al. (1999) for the Young's modulus (taken throughout this discussion as three times the shear modulus, as in incompressible material) of the cortical layer of a fibroblast adherent to a surface, 0.06–0.12 MPa, approaches, but is somewhat smaller than, our values for the stiffness of fibroblasts in a matrix. Tables 4 and 5 show that our fibroblast stiffness values are much above the range of Young's moduli reported for single leukocytes, 0.001–1.0 kPa (Sung et al., 1988; Zahalak et al., 1990), and correspondingly our fibroblast viscosity values are also much higher than those of leukocytes, 30–200 Pa-s (Sung et al., 1988; Evans and Young, 1989). Furthermore, our value of the cell viscosity, 245 kPa-s, is three orders of magnitude greater than that reported by Bausch et al. (1999) based on microrheological measurements on fibroblasts adherent to a surface. Thus it appears that the presence of a surrounding extracellular matrix greatly elevates the effective cell viscosity.

As we have appropriated a model from muscle physiology to represent nonmuscle cell mechanics, it is of interest to compare the values of the mechanical properties we have identified for fibroblasts in a collagen matrix with corresponding values for isolated, maximally activated muscle fibers (at maximum myofilament overlap). Tetanized isometric frog skeletal muscle generates a stress of ~0.25 MPa (Ford et al., 1981); thus a muscle fiber of the same cross-sectional area as our fibroblasts would generate a force of 12.5 μN, ~10 times higher than we measure. Similarly, the stiffness of frog muscle fibers subjected to step changes in length, based on the T_2 force response, is ~20 MPa (Ford et al., 1981). This is an order of magnitude higher than our value for the sum of the series and parallel cell stiffnesses. The apparent viscosity of active skeletal muscle can be estimated from the standard force-velocity curve by assuming that the *deviation* of the force from the isometric value

at any velocity is attributable to (effective) viscosity. Using Katz's (1939) data for lengthening muscle, this assumption yields an apparent viscosity of ~0.26 MPa-s, compared to our value of 0.25 MPa-s for fibroblasts. These comparisons suggest that contractile interactions may contribute significantly to the mechanical properties of elongated fibroblasts in a collagen matrix. Finally, Table 2 shows that the mean values of the passive moduli $3\mu_0$ and $3\mu_\infty$ lie in the range 4 kPa to 9 kPa. Comparing these values to the effective Young's moduli of the cells listed in Table 4, 0.09 MPa and 0.67 MPa, it appears that the apparent bulk stiffness of the individual fibroblasts is much higher than that of the surrounding matrix.

CONCLUSION

By using a combination of continuum and statistical mechanics it is possible to derive a constitutive equation for bio-artificial tissues, relating stress to deformation history, that makes explicit the separate contributions of cells and matrix. For a given matrix this constitutive relation permits us to deduce the mechanical properties of the cells from measurements on the tissue or, alternately, knowing the mechanical properties of individual cells (as well as their spatial distributions and orientations) we can predict the mechanical behavior of the composite tissue. Relaxation experiments support the general validity of the theory and yield values of cell contractile force and stiffness roughly an order of magnitude lower than corresponding properties of active skeletal muscle, whereas the cell viscosity is identified to have a value comparable to that of active skeletal muscle.

REFERENCES

Barocas, V. H., A. G. Moon, and R. T. Tranquillo. 1995. The fibroblast-populated collagen microsphere assay of cell traction force. Part 2. Measurement of the cell traction parameter. *J. Biomech. Eng.* 117: 161–170.

Barocas, V. H., and R. T. Tranquillo. 1997. An anisotropic biphasic theory of tissue equivalent mechanics: the interplay among cell traction, fibrillar network deformation, fibril alignment and cell contact guidance. *J. Biomech. Eng.* 119:137–145.

Bausch, A. R., W. Moller, and E. Sackmann. 1999. Measurement of local viscoelasticity and forces in living cells by magnetic tweezers. *Biophys. J.* 76:573–579.

Bell, E., B. Ivarsson, and C. Merrill. 1979. Production of a tissue-like structure by contraction of collagen lattices by human fibroblasts of different proliferative potential in vitro. *Proc. Natl. Acad. Sci. USA.* 76:1274–1278.

Bird, B. R., C. F. Curtiss, R. C. Armstrong, and O. Hassager. 1987. Dynamics of Polymeric Liquids, Vol. 2. Kinetic Theory. Wiley, New York. 65–66.

Darby, I., O. Skalli, and G. Gabbiani. 1990. α-Smooth muscle actin is transiently expressed by myofibroblasts during experimental wound healing. *Lab. Invest.* 63:21–29.

Eschenhagen, T., C. Fink, U. Remmers, H. Scholz, J. Wattchow, J. Weil, W. Zimmermann, H. H. Dohmen, H. Schafer, N. Bishopric, T. Wakatsuki, and E. L. Elson. 1997. Three-dimensional reconstitution of embryonic cardiomyocytes in a collagen matrix: a new heart muscle model system [In Process Citation]. *FASEB J.* 11:683–694.

Evans, E., and A. Young. 1989. Apparent viscosity and cortical tension of blood granulocytes determined by micropipette aspiration. *Biophys. J.* 56:151–160.

Ford, L. E., A. F. Huxley, and R. M. Simmons. 1981. The relation between stiffness and filament overlap in striated frog muscle fibers. *J. Physiol.* 311:219–249.

Freudenthal, A. M. 1966. Introduction to the Mechanics of Solids. Wiley, New York. 253–254.

Fung, Y. C. 1993. Biomechanics: Mechanical Properties of Living Tissues. Springer, New York. 277–280.

Glerum, J. J., R. Van Mastrigt, and A. J. Van Koeveringe. 1990. Mechanical properties of mammalian single smooth muscle cells. III. Passive properties of pig detrusor and human a terme uterus cells. *J. Muscle Res. Cell Motil.* 11:453–462.

Harris, D. E., and D. M. Warshaw. 1991. Length vs. active force relationship in single isolated smooth muscle cells. *Am. J. Physiol. Cell Physiol.* 260:C1104–C1112.

Hill, A. V. 1938. The heat of shortening and the dynamic constants of muscle. *Proc. R. Soc. B.* 126:136–195.

Intengan, H. D., L. Y. Deng, J. S. Li, and E. L. Schiffrin. 1999. Mechanics and composition of human subcutaneous resistance arteries in essential hypertension. *Hypertension.* 33:569–574.

Katz, B. 1939. The relation between force and speed of shortening in muscular contraction. *J. Physiol.* 96:45–64.

Kolodney, M. S., and E. L. Elson. 1993. Correlation of myosin light chain phosphorylation with isometric contraction in fibroblasts. *J. Biol. Chem.* 268:23850–23855.

Kolodney, M. S., and E. L. Elson. 1995. Contraction due to microtubule disruption is associated with increased phosphorylation of myosin regulatory light chain. *Proc. Natl. Acad. Sci. USA.* 92:10252–10256.

Kolodney, M. S., and R. B. Wysolmerski. 1992. Isometric contraction by fibroblasts and endothelial cells in tissue culture: a quantitative study. *J. Cell Biol.* 117:73–82.

Moon, A. G., and R. T. Tranquillo. 1993. Fibroblast-populated collagen microsphere assay of cell traction force. Part I. Continuum model. *AIChE J.* 39:163–177.

Murray, J. D., and G. F. Oster. 1984. Cell traction models for generating pattern and form in morphogenesis. *J. Mater. Biol.* 19:265–279.

Murray, J. D., G. F. Oster, and A. K. Harris. 1983. A mechanical model for mesenchymal morphogenesis. *J. Mater. Biol.* 17:125–129.

Odell, G. M., G. F. Oster, P. Alberch, and B. Burnside. 1981. The mechanical basis of morphogenesis. I. Epithelial folding and invagination. *Dev. Biol.* 85:446–462.

Sung, K. L. P., C. Dong, G. W. Schmid-Schonbein, S. Chien, and R. Skalak. 1988. Leukocyte relaxation properties. *Biophys. J.* 54:331–336.

Tranquillo, R. T. 1999. Self-organization of tissue-equivalents: the nature and role of contact guidance. *Biochem. Soc. Symp.* 65:27–42.

Tranquillo, R. T., and J. D. Murray. 1992. Continuum model of fibroblast-driven wound contraction: inflammation-mediation. *J. Theor. Biol.* 158: 135–172.

Tranquillo, R. T., and J. D. Murray. 1993. Mechanistic model of wound contraction. *Surg. Res.* 55:233–247.

Wakatsuki, T., M. S. Kolodney, G. I. Zahalak, and E. L. Elson. 2000. Cell mechanics studied by a reconstituted model tissue. *Biophys. J.* 79: 2353–2368.

Wall, F. T. 1958. Chemical Thermodynamics. Freeman, San Francisco. 339–349.

Zahalak, G. I., W. B. McConnaughey, and E. L. Elson. 1990. Determination of cellular mechanical properties by cell poking, with an application to leukocytes. *J. Biomech. Eng.* 112:283–294.